International Journal of Dynamics and Control (2021) 9:910–921
https://doi.org/10.1007/s40435-020-00727-7

In-plane vibration analysis of parabolic arches having a variable thickness

Beytullah Temel[1] · **Timuçin Alp Aslan**[1] · **Ahmad Reshad Noori**[2]

Received: 12 August 2020 / Revised: 29 October 2020 / Accepted: 31 October 2020 / Published online: 3 January 2021

Abstract
This article deals with free and forced vibration responses of the viscoelastic parabolic arches of variable thickness. Firstly, considering the effects of shear deformation and damping, time-dependent motion equations of in-plane loaded parabolic arches are obtained. Subsequently, the Laplace transform is applied to the obtained equations and solved by a powerful numerical method. Furthermore, the Kelvin viscose model is used to describe the viscoelastic material. Using an effective and suitable inverse numerical Laplace transform method, the results were transferred back to time space. The verification of the presented method is performed by comparing its results with the results of ANSYS. It has been shown in several examples that the proposed method is highly accurate and efficient compared to step-by-step time integration methods.

Keywords Laplace transform · Free vibration · Forced vibration · Kelvin damping model · Parabolic arches

1 Introduction

Rods and arches are used in many man-made structures such as bridges, roof structures, and aerospace structures. As aspects of modern architectural design, curved rods and arches of varying cross-sections are commonly used in bridges. These important practical applications of arches and curved rods have attracted the interest of researchers in determining the static and dynamic behavior of those structures.

Many researchers have studied curved beams using various methods. Among those, Haktanır [1], Bayhan [2], Bozkurt [3] and Yildirim et al. [4] investigated the static response of curved beams. The dynamic analysis of cylindrical helical rods was examined by Çalım [5]. Aktan [6] studied the free vibration of in-plane circular beams. Çoban [7] investigated the dynamic analysis of curved beams with the Gâteaux derivative. Akkurt [8] investigated the dynamic analysis of circular beams. Karaca [9] examined the in-plane and out-of-plane dynamic analysis of circular beams. The longitudinal vibrations of elastic bars were investigated by Ecer [10]. Vibration analysis of circular arches was examined by Rosa and Franciosi [11] and by Karami and Malekzadeh [12]. Dynamic analysis of straight beams was examined by Manolis and Beskos [13], Beskos and Narayanan [14] and Huang et al. [15]. The dynamic behavior of the arches of variable thickness was examined by Tong et al. [16] and Huang et al. [17]. Dynamic analysis of arches was also studied by Wu and Chiang [18], Tufekci and Arpaci [19] and Tüfekci and Özdemirci [20]. Dynamic analysis of structures in the Laplace domain was examined by Temel et al. [21], Yildirim and Tutuncu [22], Noori et al. [23] and Aslan et al. [24].

The literature survey shows that many studies dealing with static, free vibration and transient analysis of curved rods and arches have been made and several methods have been investigated by researchers [1–24]. The present study is the extension of the elastic case discussed in [21], free vibration and viscoelastic response of the arch are also examined. The CFM is a numerical solution method which transforms a two-point boundary value problem into a system of initial value problems. In this study, Butcher's RK5 method [25] is applied for the solution of initial value problems. The application of Laplace transform, with respect to time, to partial differential equations, converts them to ordinary differential equations

✉ Ahmad Reshad Noori
arnoori@gelisim.edu.tr

Beytullah Temel
btemel@cu.edu.tr

Timuçin Alp Aslan
taslan@cu.edu.tr

[1] Department of Civil Engineering, Çukurova University, Adana, Turkey

[2] Department of Civil Engineering, Istanbul Gelisim University, Istanbul, Turkey

in the transformed domain. Thus the numerical solution of partial differential equations in the Laplace domain can be done easily. A highly effective inverse Laplace transformation method has been implemented to retransfer the results to time–space. Materials of the rods are assumed to be linear elastic or viscoelastic. To demonstrate the efficiency of the proposed procedure, the transient responses of a pin-ended parabolic arch of variable thickness are presented in this article. Current results are compared with those of ANSYS [26], a finite element package which applies the Newmark time integration method to solve the time dependent equations. The advantages of the present method are high accuracy and computational time savings.

2 Governing equations

Consider an arch (Fig. 1), having a moving reference with the origin on the arch axis is defined by the unit vectors **n** (normal), **t** (tangential), **b** (binormal) (see Sokolnikoff and Redheffer [27]). The relationship between these vectors are as follows:

$$\frac{\partial \mathbf{t}}{\partial z} = \chi \mathbf{n} \tag{1}$$

$$\frac{\partial \mathbf{n}}{\partial z} = \tau \mathbf{b} - \chi \mathbf{t} \tag{2}$$

$$\frac{\partial \mathbf{b}}{\partial z} = -\tau \mathbf{n} \tag{3}$$

where τ and χ are the curvature of the arch axis. For in-plane loaded parabolic arches $\chi = \frac{1}{r(\phi)} = \frac{Cos^3\phi}{r_0}$ and $\tau = 0$. **U** is the displacement, **Ω** is rotation, **T** is the internal force, **M** is the internal moment of any point of the arch.

The components of the vectors for the in-plane loaded arches can be written as follows:

$$\mathbf{U} = U_t \mathbf{t} + U_n \mathbf{n} \tag{4}$$

$$\mathbf{\Omega} = \Omega_b \mathbf{b} \tag{5}$$

$$\mathbf{T} = T_t \mathbf{t} + T_n \mathbf{n} \tag{6}$$

$$\mathbf{M} = M_b \mathbf{b} \tag{7}$$

where T_t is the internal force in the axial direction, T_n is the shear force, M_b is the flexural moment, U_t is the tangential component of displacement, U_n is the normal component of displacement, Ω_b describes the rotation. Displacements and rotations are considered to be infinitesimal and the following equations can be obtained.

$$\frac{\partial \mathbf{U}}{\partial z} + \mathbf{t} \times \mathbf{\Omega} - \mathbf{CT} = 0 \tag{8}$$

$$\frac{\partial \mathbf{\Omega}}{\partial z} - \mathbf{DM} = 0 \tag{9}$$

$$\frac{\partial \mathbf{T}}{\partial z} + \mathbf{q} - \rho A \frac{\partial^2 \mathbf{U}}{\partial t^2} = 0 \tag{10}$$

$$\frac{\partial \mathbf{M}}{\partial z} + \mathbf{t} \times \mathbf{T} + \mathbf{m} - \rho I \frac{\partial^2 \mathbf{\Omega}}{\partial t^2} = 0 \tag{11}$$

In the above equations, ρ is the mass density of the structure, I is the moment of inertia, A is the area of cross-section of the arch, **q** is the distributed load and **m** is the distributed moment. **C** and **D** are the stiffness matrices of the structure. The infinitesimal length of the parabolic arch can be written by the curvature as below:

$$r = \frac{r_0}{Cos^3\phi} \tag{12}$$

where r_0 is the radius of curvature in the midpoint of the arch. The assumptions and related formulations of this kind of planar arches are discussed in detail by Kıral and Ertepınar [28]. By employing the above-mentioned assumptions, the governing equations of the dynamic response of parabolic arches with variable cross-section are obtained and the set of 6 partial differential equations are given below:

$$\frac{\partial U_t}{\partial \phi} = U_n + \frac{r_0}{Cos^3\phi} \frac{T_t}{EA(\phi)} \tag{13}$$

$$\frac{\partial U_n}{\partial \phi} = -U_t + \frac{r_0}{Cos^3\phi} \Omega_b + \frac{r_0}{Cos^3\phi} \frac{T_n \alpha_n}{GA(\phi)} \tag{14}$$

$$\frac{\partial \Omega_b}{\partial \phi} = \frac{M_b}{EI_b(\phi)} \frac{r_0}{Cos^3\phi} \tag{15}$$

$$\frac{\partial T_t}{\partial \phi} = \frac{r_0}{Cos^3\phi} \rho A(\phi) \frac{\partial^2 U_t}{\partial t^2} + T_n - p_t \frac{r_0}{Cos^3\phi} \tag{16}$$

$$\frac{\partial T_n}{\partial \phi} = \frac{r_0}{Cos^3\phi} \rho A(\phi) \frac{\partial^2 U_n}{\partial t^2} - T_t - p_n \frac{r_0}{Cos^3\phi} \tag{17}$$

$$\frac{\partial M_b}{\partial \phi} = \frac{r_0}{Cos^3\phi} \rho I_b(\phi) \frac{\partial^2 \Omega_b}{\partial t^2} - T_n \frac{r_0}{Cos^3\phi} - m_b \frac{r_0}{Cos^3\phi} \tag{18}$$

In the above equations, ϕ is independent variable, E is the modulus of elasticity, $h(\phi)$ is the thickness of the arch, $A(\phi)$ is the area of cross-section of the arch, $I_b(\phi)$ is area moment of inertia, α_n is the shear correction factor for first order shear deformation theory, p_t is the external axial load, p_n is the external normal load and m_b is the external bending moment.

The column matrix of unknowns,
$\{\mathbf{Y}(\phi, t)\}$, can be written as follows:

$$\{\mathbf{Y}(\phi, t)\} = \{U_t, U_n, \Omega_b, T_t, T_n, M_b\}^T \tag{19}$$

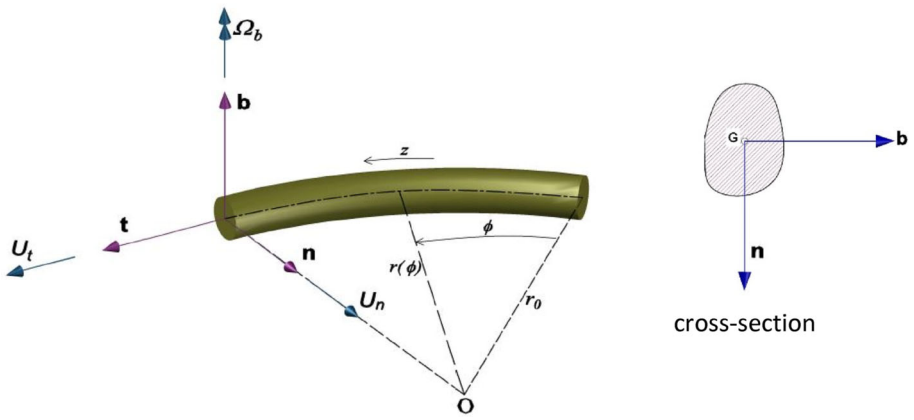

Fig. 1 Geometry of the arch

In this study, the Kelvin damping model is used for the analysis of viscoelastic status (See Boley and Weiner [29]). When performing damped forced vibration analysis, Laplace transformation of material constants E and G will be as follows:

$$E_v = E(1+gs), \quad G_v = G(1+gs) \tag{20}$$

where E_v and G_v are viscoelastic constants of material, and s is the Laplace transform parameter (see Temel et al. [30]). By using the Laplace transform, Eqs. (13–18) can be converted to ordinary differential Eqs. (21–26), which govern the viscoelastic response of considered structures.

$$\frac{d\overline{U}_t}{d\phi} = \overline{U}_n + \frac{r_0}{Cos^3\phi}\frac{\overline{T}_t}{E_v A(\phi)} \tag{21}$$

$$\frac{d\overline{U}_n}{d\phi} = -\overline{U}_t + \overline{\Omega}_b\frac{r_0}{Cos^3\phi} + \frac{r_0}{Cos^3\phi}\frac{\overline{T}_n\alpha_n}{G_v A(\phi)} \tag{22}$$

$$\frac{d\overline{\Omega}_b}{d\phi} = \frac{r_0}{Cos^3\phi}\frac{\overline{M}_b}{E_v I_b(\phi)} \tag{23}$$

$$\frac{d\overline{T}_t}{d\phi} = \frac{r_0}{Cos^3\phi}s^2\rho A(\phi)\overline{U}_t + \overline{T}_n - \overline{p}_t\frac{r_0}{Cos^3\phi} \tag{24}$$

$$\frac{d\overline{T}_n}{d\phi} = \frac{r_0}{Cos^3\phi}s^2\rho A(\phi)\overline{U}_n - \overline{T}_t - \overline{p}_n\frac{r_0}{Cos^3\phi} \tag{25}$$

$$\frac{d\overline{M}_b}{d\phi} = \frac{r_0}{Cos^3\phi}s^2\rho I_b(\phi)\overline{\Omega}_b - \overline{T}_n\frac{r_0}{Cos^3\phi} - \overline{m}_b\frac{r_0}{Cos^3\phi}$$

where the terms shown by ($\overline{\bullet}$) indicate the Laplace transform of the related quantities.

The Laplace transformation of axial, flexural and mass moment of inertia are given as:

$$L\left[\rho A(\phi)\frac{\partial^2 U_t}{\partial t^2}\right] = \rho A(\phi)\left[s^2\overline{U}_t - sU_t(\phi,0) - \frac{\partial U_t(\phi,0)}{\partial t}\right]$$

$$L\left[\rho A(\phi)\frac{\partial^2 U_n}{\partial t^2}\right] = \rho A(\phi)\left[s^2\overline{U}_n - sU_n(\phi,0) - \frac{\partial U_n(\phi,0)}{\partial t}\right]$$

$$L\left[\rho I_b(\phi)\frac{\partial^2 \Omega_b}{\partial t^2}\right] = \rho I_b(\phi)\left[s^2\overline{\Omega}_b - s\Omega_b(\phi,0) - \frac{\partial \Omega_b(\phi,0)}{\partial t}\right] \tag{27}$$

The last two terms on the right-hand side of Eq. (27) are initial conditions and are taken as 0 in this study. Matrix notation of Eqs. (21–26) can be written as follows:

$$\frac{d\{\overline{\mathbf{Y}}(\phi,s)\}}{d\phi} = [\overline{\mathbf{A}}(\phi,s)]\{\overline{\mathbf{Y}}(\phi,s)\} + \{\overline{\mathbf{F}}(\phi,s)\} \tag{28}$$

The RK5 algorithm is used for the solution of the initial-value problem based on the CFM (see Temel et al. [21] and Temel and Noori [31]).

3 Numerical examples and discussion

Program code has been prepared with the aid of FORTRAN in order to examine the free and damped forced vibration of variable thickness parabolic arches with the proposed method. CFM and Laplace transform are used together to solve the equations that govern the dynamic behavior of the arch. In order to retransfer the results obtained by the Laplace transform to the time space, the modified Durbin inverse transfer method, which is a very effective inverse Laplace transform, has been applied (see Durbin [32] and Temel and Şahan [33]). By virtue of the fact that there is a lack of results in the available literature for the present class problems, analysis results are compared with those of ANSYS.

At first, the natural frequencies of a pin-ended isotropic parabolic arch with a variable cross section, shown in Fig. 2a, are obtained and compared with the results of ANSYS. In order to achieve consistent results with finite elements, it is necessary to define approximately variable cross-sectional properties along the arch axis. Therefore, it is necessary to divide the problem into a sufficient number of elements. In the presented study the natural frequencies of the considered structure are listed in Table 1 for a various number of tapered sections. It can be clearly seen that at least 50 tapered beam Sects. (100 elements of BEAM54) must be defined in ANSYS to describe an approximately continuous variable thickness along the axis. Whereas by using the current

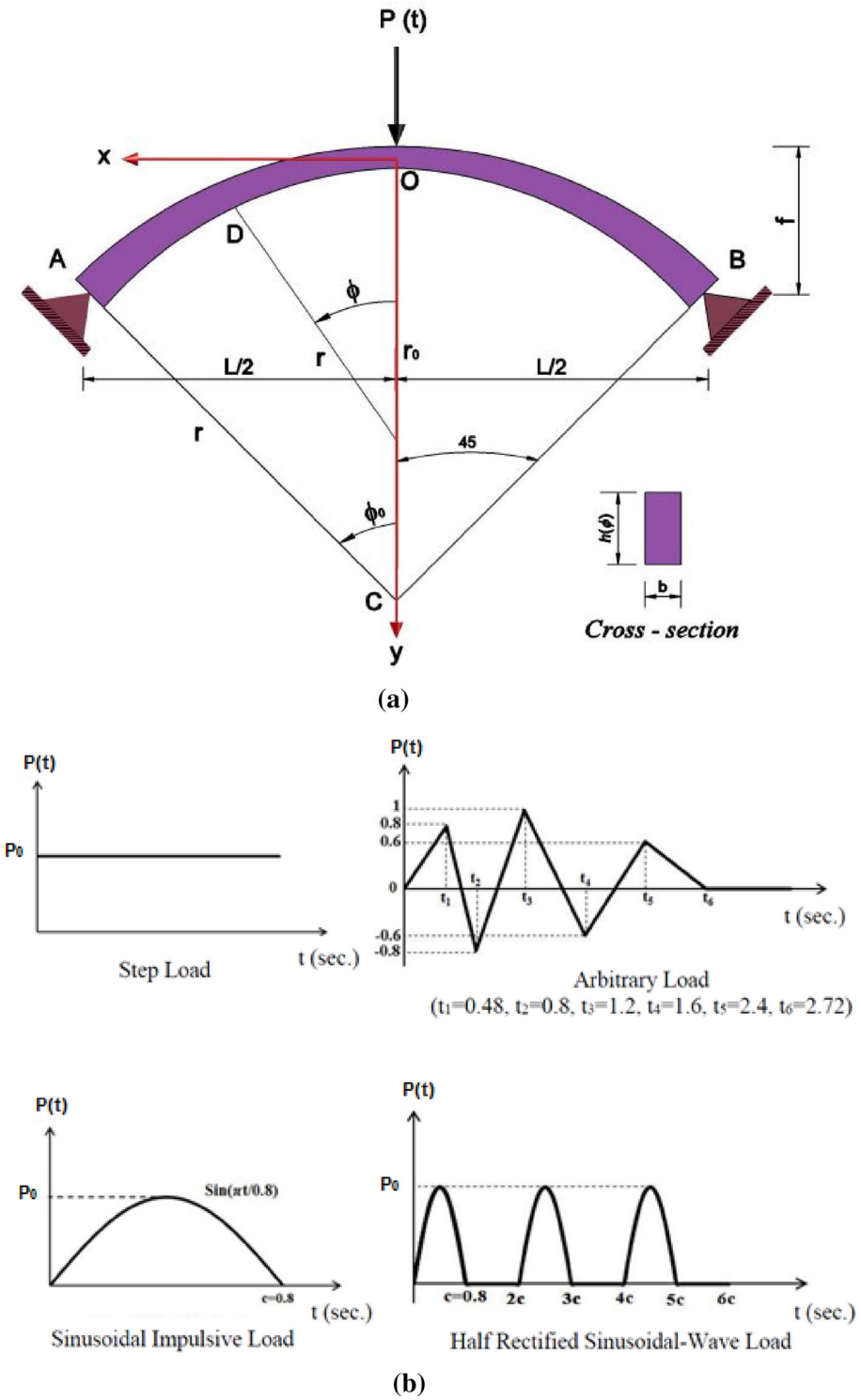

Fig. 2 (**a**) Pin-ended parabolic arch; (**b**) Dynamic loads

method, cross-sectional area of the arch varies with the curvature of the arch. Comparisons given in Table 1 show that current results are in good agreement with the results of the finite element method.

After the free vibration analysis, the forced vibration analysis of the structure discussed will now be examined for a point dynamic load applied to its crown point. Material properties are: Poisson's ratio, $\nu = 0.3$, mass density, $\rho = 7850 \times 10^{-6}$ kg/cm^3, and modulus of elasticity, $E = 2.1 \times 10^6$ kgf/cm^2. Four functions of dynamic loads, shown in Fig. 2b, with the amplitude $P_0 = 1$ *kgf*, are applied on the midpoint of the structure. Equation of the axis line of

Table 1 First ten natural frequencies of the pin-ended parabolic arch of variable thickness (Hz)

Mod	ANSYS (50 elements)	ANSYS (100 elements)	ANSYS (200 elements)	Present study
1	1.375	1.373	1.373	1.371
2	3.968	3.965	3.965	3.959
3	7.856	7.853	7.854	7.836
4	13.032	13.026	13.026	12.983
5	18.850	18.773	18.772	18.748
6	19.682	19.672	19.673	19.631
7	27.312	27.289	27.289	27.132
8	36.426	36.323	36.324	36.046
9	46.745	46.641	46.641	46.189
10	58.431	58.232	58.233	57.534

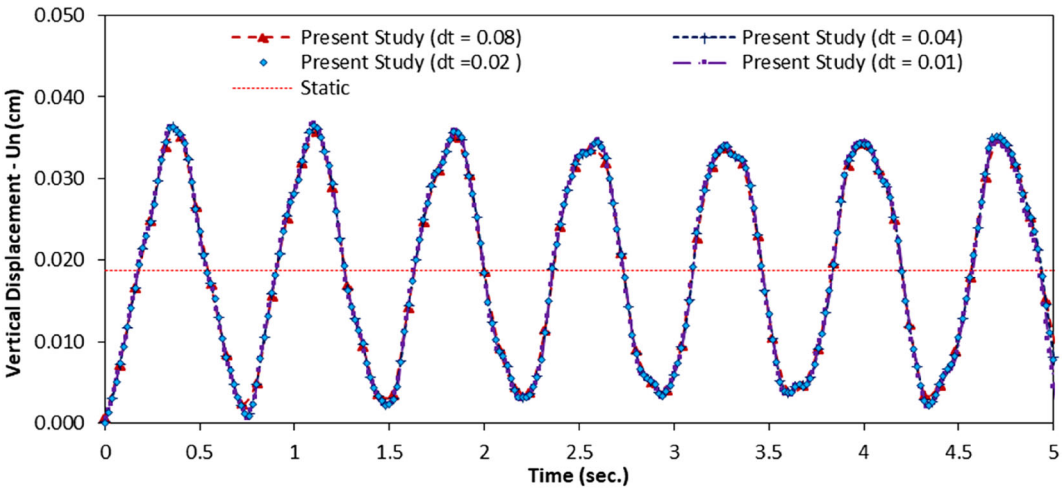

Fig. 3 Deflection of the arch Crown Point

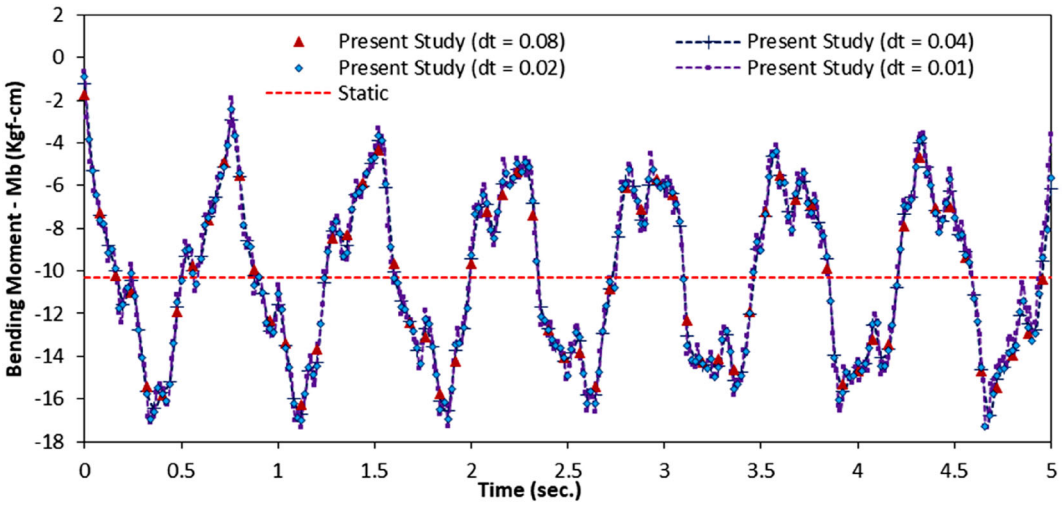

Fig. 4 Moment of bending of the arch Crown Point

the parabolic arch in the x, y coordinate system and its radius of curvature or "r" along the axis are as follows:

$$y = \frac{4fx^2}{L^2}, \quad r = \frac{r_0}{Cos^3\phi}$$

where $r = r_0 Cos^3\phi$ is the radius of curvature of the midpoint of the arch (point O).

$$r_0 = \frac{L^2}{8f}$$

The cross-section of the arch is assumed to have a constant width and a variable thickness, given as below.

$$b(\phi) = b(0); \quad h(\phi) = \frac{h(0)}{\cos\phi}$$

Here the flexural rigidity and cross sectional area of arch are variable.

$$EI_b(\phi) = E\frac{bh^3(\phi)}{12}; \quad A(\phi) = bh(\phi)$$

The boundary conditions are as follows:

$$\phi = 0 \rightarrow \begin{cases} U_t = 0 \\ \Omega_b = 0 \\ T_n = -P/2 \end{cases} \qquad \phi = \phi_0 \rightarrow \begin{cases} U_t = 0 \\ U_n = 0 \\ M_b = 0 \end{cases}$$

The Eqs. (21–26) are solved numerically by the CFM in the Laplace domain. Current results are compared with those of finite element software, which uses the conventional step by step Newmark time integration method to solve the equations of motion. Comparisons are demonstrated in the graphics. Shear deformation is considered in this problem. The geometric properties of the parabolic arch are given below:

$$\begin{aligned} &b = 1 \text{ cm}; \quad h(0) = 1 \text{ cm}; A(0) \\ &\quad = 1 \text{ cm}^2; \quad I_b(0) = 0.0833cm^4; \\ &L = 200 \text{ cm}; \quad r_0 = 100 \text{ cm}; \quad f = 50 \text{ cm} \\ &P_0 = 1\ kgf; \quad \phi_0 = 45^\circ; \quad \alpha_n = 1.2 \end{aligned}$$

Closed-form of the Laplace transforms of the considered dynamic loads are available in the literature. Comparison of the vertical displacement and bending moment of the crown point of the considered structure for step load function is given in Figs. 3 and 4. The material of the parabolic arch is considered to be isotropic-elastic.

The problem has been solved for various time increments as transform parameters ($N = 64$, $dt = 0.08$ s.), ($N = 128$, $dt = 0.04$ s.), ($N = 256$, $dt = 0.02$ s.) and ($N = 512$, $dt = 0.01$ s.). As is evident in the comparisons, the results obtained for fewer Laplace parameters and more Laplace parameters overlap. This comparison shows that the proposed method is highly effective and efficient. The parabolic arch is divided into 100 uniaxial elements in ANSYS while the cross section of the arch is considered to be variable.

Figures 5 and 6 show the vertical displacement and M_b bending moment results at the mid span of the parabolic arch obtained via ANSYS.

The comparisons of the current results and those of the Newmark method for various time steps given in Figs. 7 and 8 show the U_n deflection and M_b bending moment at the midpoint of the arch for a step load.

For this example, the time increment must be at least 0.005 s to achieve consistent results in the ANSYS package program. However, with the proposed approach, results with the same precision can be achieved using a coarse time increment of 0.08 s. This leads to considerable savings in computation time (see Temel and Şahan [33]).

Viscoelastic analysis is now performed for various damping-ratios. Comparisons of vertical displacement U_n and bending moment M_b versus time at the arch midpoint for step load are given in Figs. 9 and 10. In the figures given, a comparison of the results obtained with the approach presented and ANSYS is given. In this example, it is seen that the results obtained by taking the dt = 0.08 s with the proposed method coincide with the results obtained using a finer time increment dt = 0.005 s in ANSYS.

Vertical displacement U_n and bending moment M_b versus time at the arch midpoint under the sinusoidal load and arbitrary load shown in Fig. 2b are shown in Figs. 11, 12, 13 and 14 respectively. The Laplace transform of the arbitrary load is performed using a piecewise linear approach given by Narayanan [34].

The parabolic arch is now considered under a half rectified sinusoidal-wave load shown in Fig. 2b. The vertical displacement U_n and bending moment M_b results versus time are given for a period of 8 s. in Figs. 15 and 16. Solutions are obtained for both elastic and viscoelastic cases.

For a better interpretation of the amplitude of vibration under the periodic sinusoidal-wave loading the vertical displacement and bending moment is given for 24 s. in Figs. 17 and 18.

The beating can be clearly seen in Figs. 17 and 18. The reason for this is that the frequency of the periodic sinusoidal wave load (1.250 Hz) is very close to the natural vibration frequency value of the structure (1.371 Hz). When the wall clock time is compared it can be clearly observed that using the presented scheme leads to considerable saving in computation time. The suggested unified approach completes the related calculations approximately 208 times quicker than the finite element software, ANSYS, for the transient response of present class problems. In ANSYS only nodal degrees of

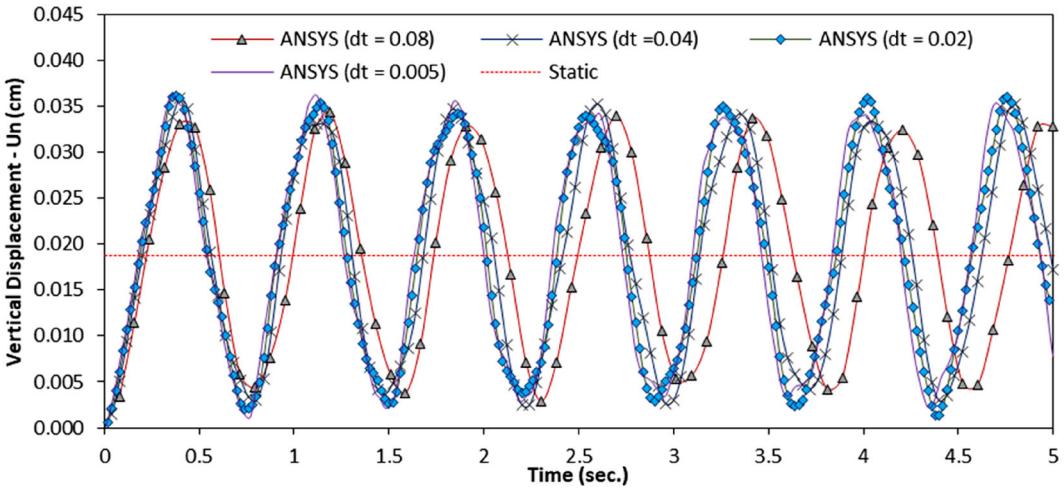

Fig. 5 Deflection of the arch Crown Point

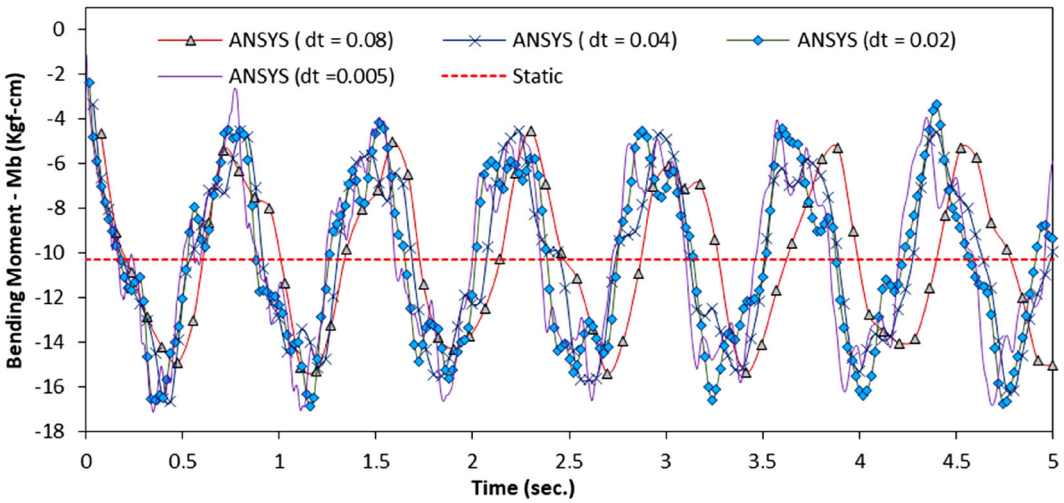

Fig. 6 Moment of bending of the arch Crown Point

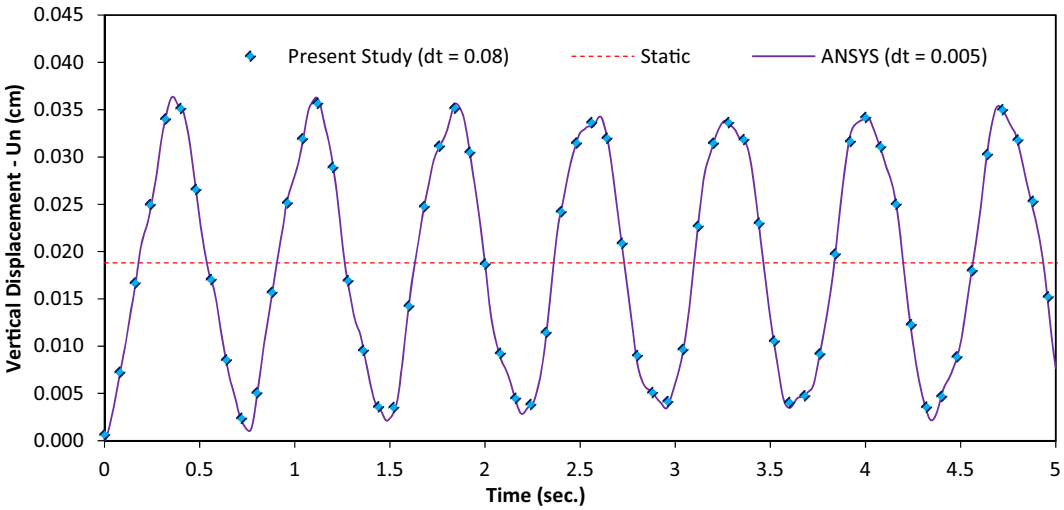

Fig. 7 Comparison of the deflection of the arch Crown Point

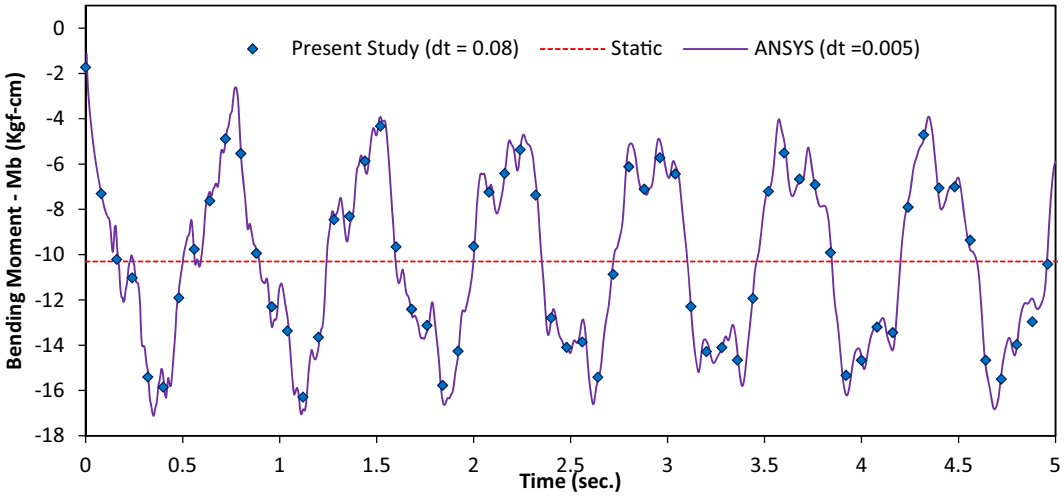

Fig. 8 Comparison Moment of bending of the arch Crown Point

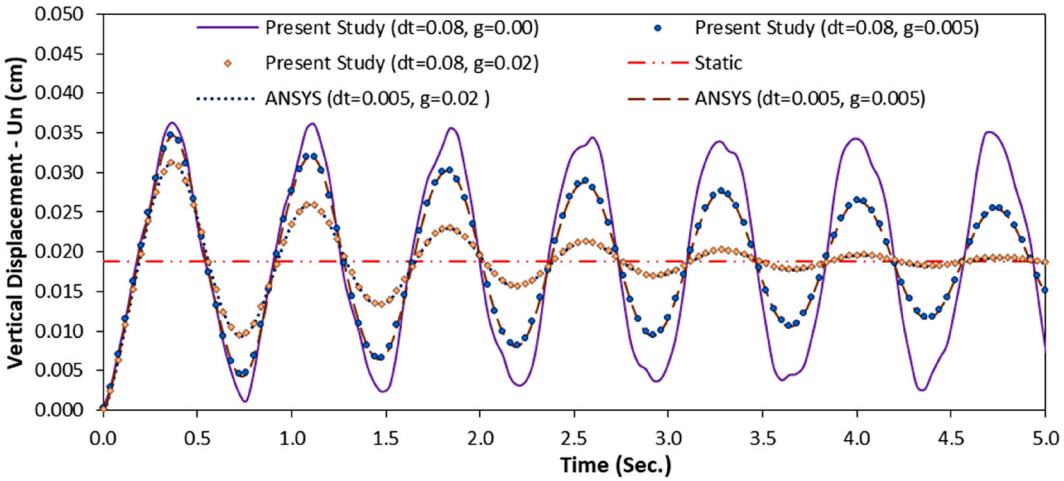

Fig. 9 Deflection of the arch Crown Point for various damping ratios

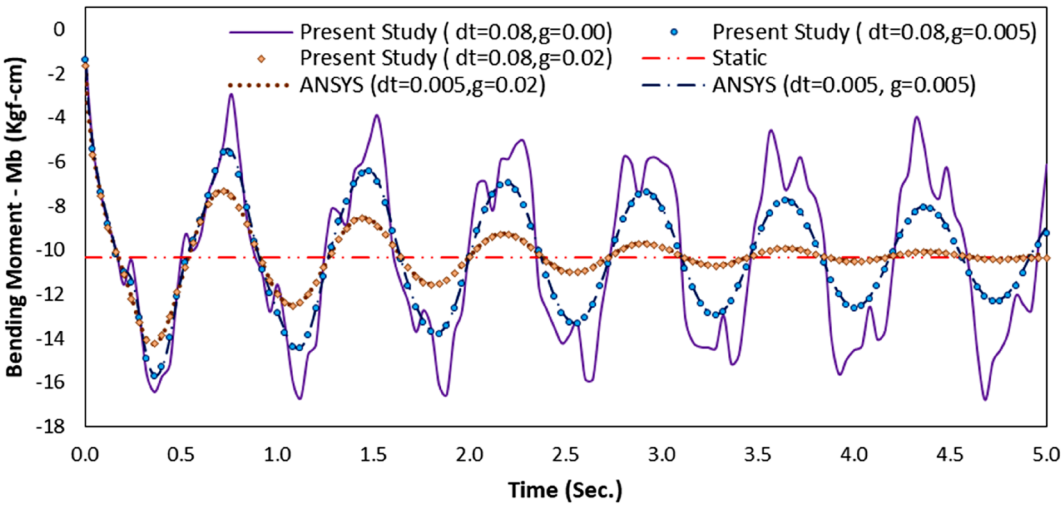

Fig. 10 Moment of bending of the arch Crown Point for various damping ratios

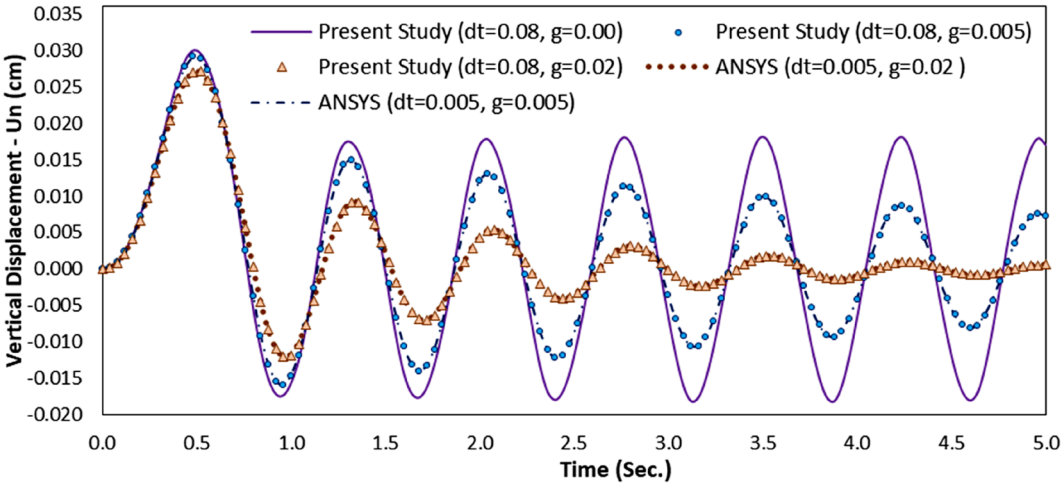

Fig. 11 Deflection of the arch Crown Point for various damping ratios

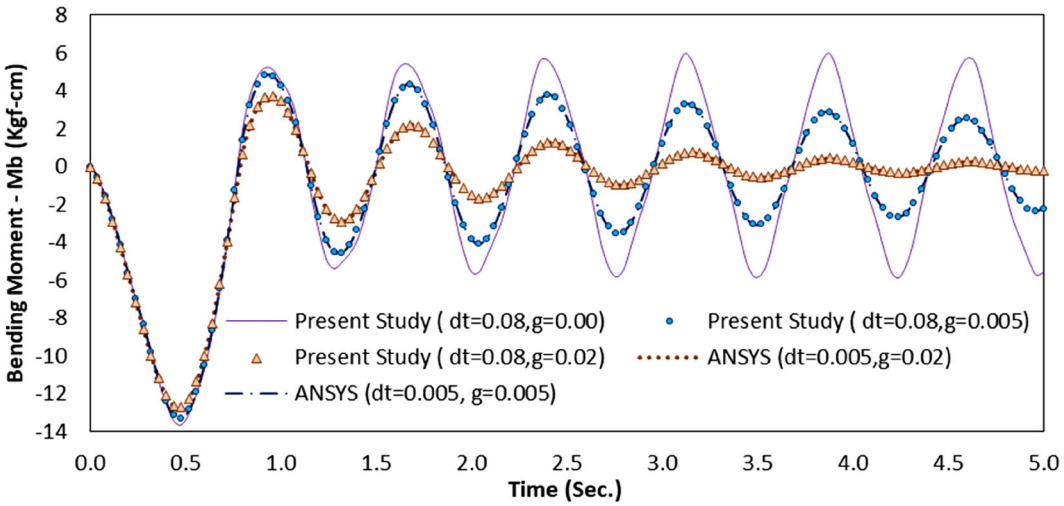

Fig. 12 Moment of bending of the arch Crown Point for various damping ratios

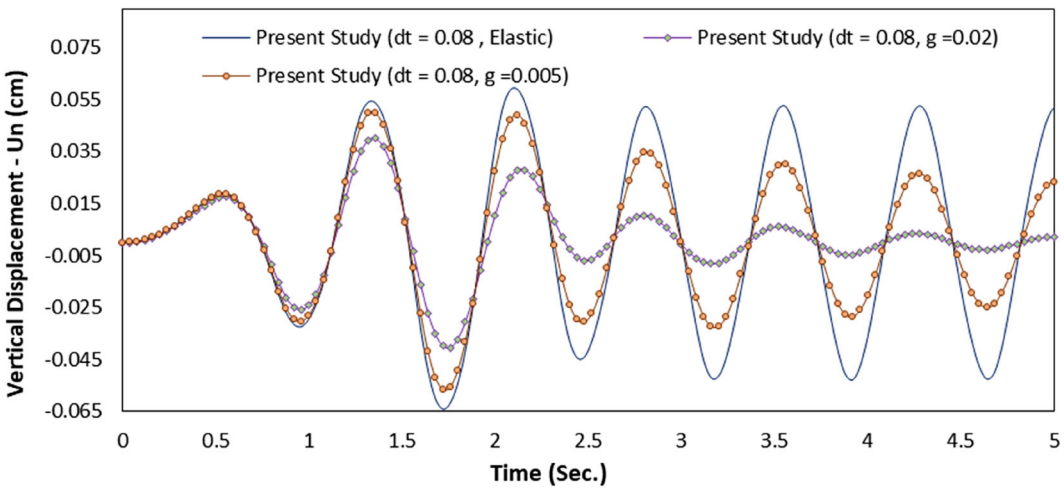

Fig. 13 Deflection of the arch Crown Point for various damping ratios

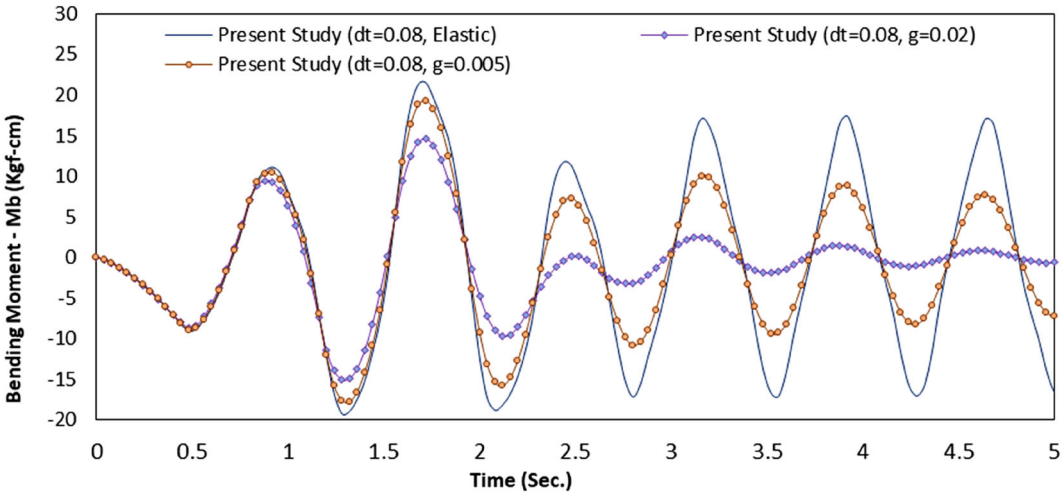

Fig. 14 Moment of bending of the arch Crown Point for various damping ratios

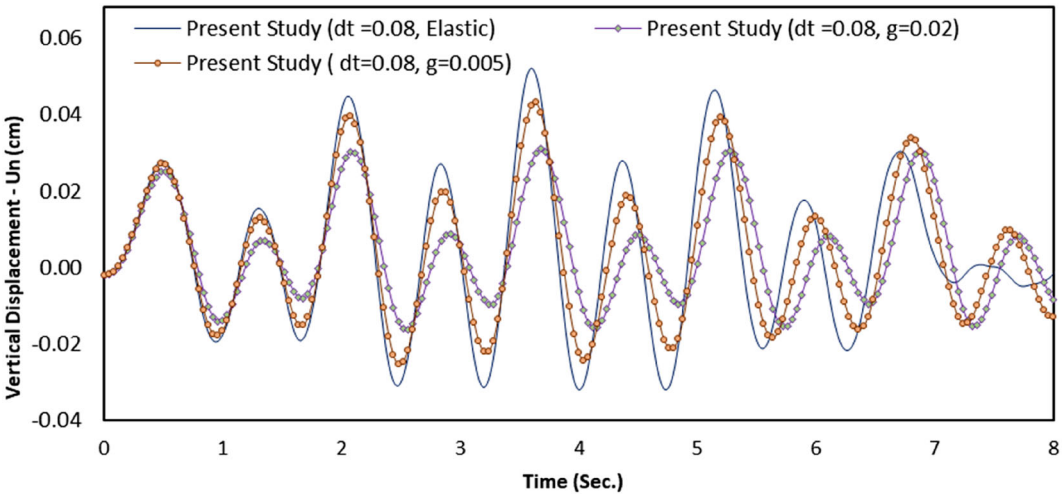

Fig. 15 Deflection of the arch Crown Point for various damping ratios

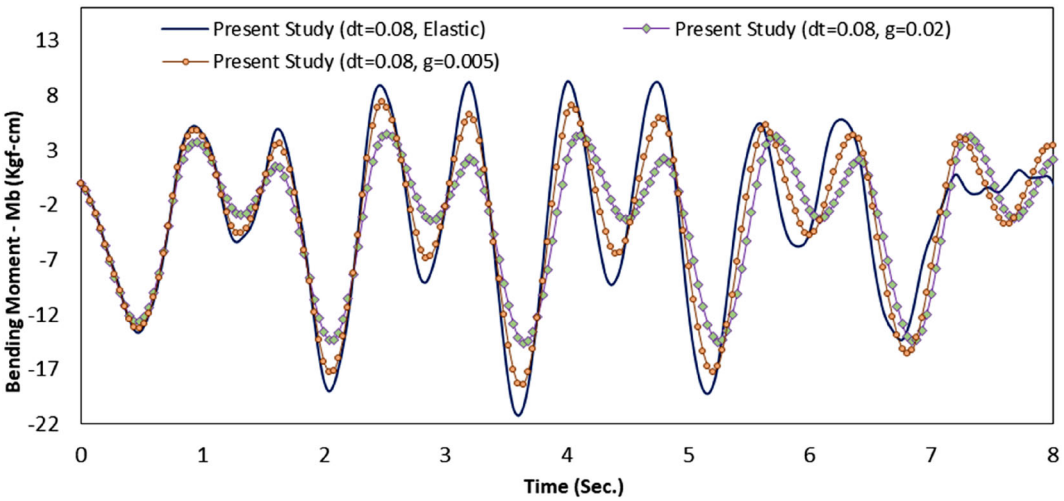

Fig. 16 Moment of bending of the arch Crown Point for various damping ratios

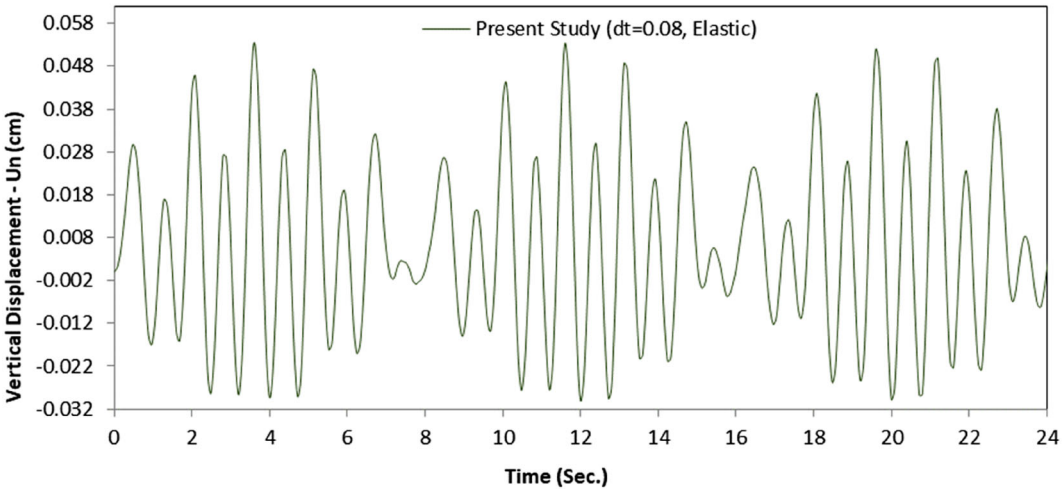

Fig. 17 Deflection of the arch Crown Point

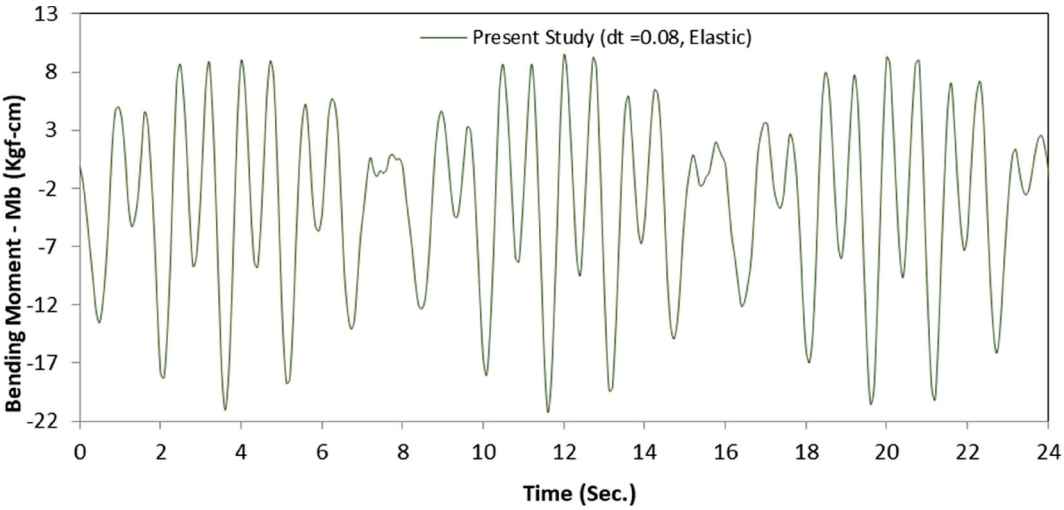

Fig. 18 Moment of bending of the arch Crown Point

freedom and element solutions are calculated (see Noori et al. [35]).

4 Conclusions

In this study, the free and forced vibrations of isotropic parabolic arches with variable thickness made of linear elastic or viscoelastic material are examined theoretically. The proposed method is a combination of the Laplace transform and the CFM. The first order shear deformation effect and damping effect are considered. RK5 algorithm is used for the numerical solution of the CFM based initial values problems. The equations governing the dynamic behavior of the arches are obtained in the time domain based on the first order shear deformation theory. The obtained equations are transferred to Laplace space with the help of Laplace transform. These ordinary differential equations are solved numerically by applying the CFM in Laplace space.

The solutions obtained are transformed into the time domain using an appropriate inverse numerical Laplace transform method. Owing to Laplace transform, a dynamic problem is reduced to a static one. Furthermore, the damping effect can be easily incorporated in the transformed domain. In order to examine the free vibration behavior of the considered arches, all external loads are equalized to zero, then the Laplace parameter "s" is replaced by a complex number "iω". Mass of the structure can be assumed to be distributed by using this unified approach, for this reason, the natural frequencies are much more accurate than those of the finite element method.

Whereas, in the forced vibration analysis the accuracy of the results of the Newmark method depends on the appropriate selection of the optimum time increment. By using the

presented method, highly accurate results can be obtained, even with a coarse time step size. The proposed unified approach is shown to be more effective and accurate than step-by-step integration methods.

Under the rectified sinusoidal wave load, it seems that the frequency of the arch is close to the frequency of the load, thus the beating phenomenon is observed in the related graphics. Additionally, this type of dynamic loads causes the shifting of oscillating periods in viscoelastic cases.

Laplace transformation gives a time-independent boundary-value problem in spatial coordinates which is then solved by the CFM. The numerical examples have proved that the suggested procedure is highly accurate and efficient, and it can be easily applied to the parabolic arches with varying section and curvature.

6. References

1. Haktanir V (1994) "A new method for the element stiffness matrix of arbitrary planar" bars. Comput Struct 52(4):679–691
2. Bayhan S (1993) Analysis of planner curved rods by stiffness matrix and transfer matrix method, MSc. Thesis, University of Cukurova, Adana, (**in Turkish**)
3. Bozkurt M (1995) The analysis of cylindrical vaults, circular and helicoidal structural systems by the complementary functions method-mathematica applications, MSc. Thesis, University of Cukurova, Adana, (**in Turkish**)
4. Yildirim V, İnce N, Kiral E (1997) Statistical analysis of compound planar frames of straight and circular members. J Eng Environ Sci 21(3):137–148.
5. Çalım FF (2003) Dynamic analysis of viscoelastic, anisotropic curved spatial rod systems. PhD. Thesis, University of Cukurova, Adana (**in Turkish**).
6. Aktan H (2008) In-plane dynamic analysis of circular beams. MSc. Thesis, Istanbul Technical University, Istanbul (**in Turkish**)
7. Çoban M (2008) Out-of-plane dynamic analysis of curved beams using mixed finite element method. MSc. Thesis, Istanbul Technical University, Istanbul, (**in Turkish**)
8. Akkurt FG (2011) Dynamic analysis of straight and circular rods on elastic foundation, MSc. Thesis, University of Mustafa Kemal, Hatay, (**in Turkish**)
9. Karaca N (2014) Static and dynamic analysis of planar rods by the transfer and stiffness matrix methods, MSc. Thesis, University of Mustafa Kemal, Hatay, (**in Turkish**)
10. Ecer S (2015) Longitudinal vibration analysis of straight bars using mixed finite element method, MSc. Thesis, Istanbul Technical University, Istanbul (**in Turkish**)
11. De Rosa MA, Franciosi C (2000) Exact and approximate dynamic analysis of circular arches using DQM. Int J Solids Struct 37:1103–1117
12. Karami G, Malekzadeh P (2004) In-plane free vibration analysis of circular arches with varying cross-sections using differential quadrature method. J Sound and Vib 274:777–799
13. Manolis GD, Beskos DE, (l982) Dynamic response of framed underground structures. Comput Struct 15(5):521–531
14. Beskos DE, Narayanan GV (l983) Dynamic response of frameworks by numerical laplace transform Comput Method Appl Mech Eng 37(3):289–307
15. Huang CS, Teng TJ, Leissa AW (1996) An accurate solution for the in-plane transient response of a circular arch. J Sound Vib 196(5):595–609
16. Tong X, Mrad N, Tabarrok B (1998) In-plane vibration of circular arches with variable cross-sections. J Sound Vib 212(1):121–140
17. Huang CS, Tseng YP, Lin CJ (1998) In-plane transient responses of arch with variable curvature using dynamic stiffness method. J Eng Mech 124:826–835
18. Wu JS, Chiang LK (2004) A new approach for free vibration analysis of arches with effects of shear deformation and rotary inertia considered. J Sound Vib 277:49–71
19. Tüfekci E, Arpacı A (1998) Exact solution of in-plane vibrations of circular arches with account taken of axial extension, transverse shear and rotatory inertia effects. J Sound Vib 209(5):845–856
20. Tüfekci E, Özdemirci Ö (2006) Exact solution of free in-plane vibration of a stepped circular arch. J Sound Vib 295:725–738
21. Temel B, Aslan TA, Noori AR (2017) An efficient dynamic analysis of planar arches. Eur Mech Sci 1(3):82–88
22. Yildirim S, Tutuncu N (2018) Axisymmetric plane vibration analysis of polar-anisotropic disks. Compos Struct 194:509–515
23. Noori AR, Aslan TA, Temel B (2018a) An efficient approach for in-plane free and forced vibrations of axially functionally graded parabolic arches with nonuniform cross section. Compos Struct 200:701–710
24. Aslan TA, Noori AR, Temel B (2018) Dynamic response of viscoelastic tapered cycloidal rods. Mech Res Commun 92:8–14
25. Chapra SC, Canale RP (1998) Numerical Methods for engineers with programming and software applications. McGraw-Hill Books, New York
26. ANSYS Swanson Analysis System, Inc., 201 Johnson Road, Houston, PA15342–1300, USA.
27. Sokolnikoff IS, Redheffer RM (1958) Mathematics of physics and modern engineering. McGraw-Hill, Tokyo
28. Kıral E, Ertepınar A (1974) Studies on elastic rods subjected to diverse external agencies part II planar rods on an elastic foundation. METU J Pure Appl Sci 7(1):41–53
29. Boley BA, Weiner JH (1960) Theory of thermal stresses. Wiley, New York
30. Temel B, Çalim FF, Tütüncü N (2004) Quasi-static and dynamic response of viscoelastic helical rods. J Sounds Vib 271:921–935
31. Temel B, Noori AR (2019) Out-of-plane vibrations of shear-deformable AFG cycloidal beams with variable cross section. Appl Acoust 155:84–96
32. Durbin F (1974) Numerical inversion of laplace transforms: an efficient improvement to Dubner and Abate's Method. Comput J 17:371–376
33. Temel B, Şahan MF (2013) Transient analysis of orthotropic, viscoelastic thick plates in the laplace domain. Eur J Mech A/Solids 37:96–105
34. Narayanan GV (1979) Numerical operational methods. In structural dynamics", Phd Thesis, University Of Minnesota, Minneapolis.
35. Noori AR, Aslan TA, Temel B (2018b) Damped transient response of in-plane and out-of-plane loaded stepped curved rods. J Braz Soc Mech Sci Eng 40:28